Published in final edited form as:

Proc SPIE Int Soc Opt Eng. 2022 ; 11942: . doi:10.1117/12.2608283.

Dehydration imaging of dental fluorosis at 1950 nm

Filipp Kashirtsev, **John Tressel**, **Daniel Fried**

University of California, San Francisco, San Francisco, CA 94143-0758

Abstract

Dental fluorosis is an increasing problem in the U.S. due to excessive exposure to fluoride from the environment. Fluorosis causes hypomineralization of the enamel during tooth development and mild fluorosis is visible as faint white lines on the tooth surface while the most severe fluorosis can result in pitted surfaces. It is difficult to differentiate lesions due to fluorosis from those due to caries. Dental fluorosis appears with extremely high contrast at short wavelength infrared (SWIR) wavelengths of 1450 and 1960 nm coincident with higher water absorption. In this study reflectance measurements at 1450 and 1950 nm were used to monitor the dehydration dynamics of lesions due to fluorosis on extracted teeth. The dehydration dynamics were compared with the lesion structure that was measured with microCT. Sixteen extracted teeth with suspected fluorosis were imaged and microCT showed that the mean surface zone thickness was 118 ± 30 μm and the lesion depth was 284 ± 105 μm for the areas of fluorosis investigated. The dehydration dynamics of lesions due to fluorosis appeared most similar to those of arrested caries lesions. There was no significant correlation (P >0.05) of the intensity change and rate of the intensity change at 1450 or 1950 nm with either the lesion surface zone thickness or the lesion depth.

Keywords

dental fluorosis; SWIR imaging; dehydration imaging; optical coherence tomography

1. INTRODUCTION

With the increase of fluoride use, the prevalence of dental caries has been reduced, but fluorosis has become a growing problem. Fluorosis is the hypomineralization of enamel due to fluoride ingestion during tooth development (first 6 years of life for most permanent teeth). Enamel fluorosis is characterized by greater surface and subsurface porosity [1]. Severe fluorosis can be readily distinguished, but the more common mild fluorosis can be easily mistaken for early enamel demineralization due to caries. Since fluorosis appears on areas of the tooth that are not common plaque accumulation sites such as tooth facial or buccal surfaces, white areas on those surfaces are assumed to be hypomineralization. The CDC published a report in August 2005 showing a 9% higher prevalence of fluorosis in American children than was found in a similar study 20 years ago [2]. Currently, fluorosis is scored based on color and tooth morphology commonly using the Thylstrup-Fejerskov (TF) index or Dean's Fluorosis Index [1]. Most cases of fluorosis can be identified using these criteria. However, it has not been confirmed that the pattern and distribution of the lesions due to fluorosis are a unique occurrence. Angmar-Mansson et al. [3] researched several optical techniques for improving the assessment of dental fluorosis. Mild enamel

fluorosis is characterized clinically by diffuse opacities [3]. The appearance is due to optical properties of a subsurface or surface porous layer with lower mineral content. These areas usually have texture and color similar to those of initial caries lesions but generally another shape and location [3]. Quantitative light-induced fluorescence (QLF) has been used as a potential diagnostic tool for fluorosis since the subsurface porosities scatter light in a similar manner to demineralized carious lesions [4]. McGrady et al. [5, 6] employed QLF in an epidemiological fluorosis survey in fluoridated and non-fluoridated communities in England and Thailand. In the epidemiological fluorosis survey carried out by McGrady et al. [5] using QLF, extrinsic stain was the most common confounding factor identified. Since images acquired using SWIR reflectance measurements are free of interference from stains beyond 1150 nm, the lesion contrast may provide a more quantitative measure of demineralization which may be advantageous for screening large numbers of teeth in epidemiological studies. Hirasuna et al. [7] reported SWIR images and polarization sensitive optical coherence tomography (PS-OCT) images of teeth at 1300 nm with fluorosis and showed that these methods can be used to characterize hypomineralization or developmental defects. OCT is ideally suited for measuring the subsurface structure of fluorotic lesions for quantifying their severity. OCT measurements of the subsurface structure of fluorotic lesions are also useful for clinical diagnosis and treatment. Measurements of the depth of hypomineralization with OCT can inform the clinician whether physical or chemical abrasion of the lesion for aesthetic reasons is likely to be successful without removing an excessive thickness of enamel. For example, if the OCT scan shows that the area of hypomineralization is quite severe and penetrates more than halfway through the enamel, it is likely that removal would result in excessive loss of tooth structure and should not be attempted. OCT measurements of the zone of higher mineral content can also be used to assess the susceptibility of the fluorotic lesion to further erosion and decay. Lesions with a thick transparent surface zone are likely more resistant to further erosion, decay and cavitation than lesions in which the hypomineralized body of the fluorotic lesion is exposed at the tooth surface.

SWIR reflectance imaging has been exploited for caries detection because sound enamel is transparent in the SWIR and the scattering coefficient increases significantly with increasing mineral loss [8–15]. Zakian et al. [16] carried out SWIR reflectance measurements from 1000–2500 nm using a hyperspectral imaging system and showed that the reflectance from sound tooth structure decreases at longer wavelengths where water absorption is higher. Further measurements over the past ten years have shown that the contrast between sound and demineralized enamel continues to increase with increasing wavelength [10, 12] due to the decreasing scattering coefficient of sound enamel [9], increased water absorption and decreased interference from stains [11]. Recent measurements have been extended to 1950 nm where extremely high contrast of demineralization has been observed [9, 11, 17]. Last year we showed that the contrast of hypomineralization on tooth surfaces at these longer SWIR wavelengths at 1450 and 1950 nm wavelengths coincident with water absorption is extremely high [18, 19].

One characteristic of lesions due to fluorosis or hypomineralization is that the lesions often have a distinct transparent surface zone that is visible in OCT images. Past studies have shown that not all lesions had completely transparent surface zones in OCT images [19, 20]

however we noticed that all the lesions due to fluorosis that were visible in microCT images had surface zones of higher mineral content. When lesions become arrested by mineral deposition, or remineralization, in the outer layers of the lesion, the diffusion of fluids into the lesion is inhibited. Hence, the rate of water diffusion out of the lesion reflects the degree of lesion activity. Previous studies have demonstrated that the optical changes due to the loss of water from porous lesions can be exploited to assess lesion severity and activity with fluorescence, thermal, and SWIR imaging [21–31]. The relationship between surface zone thickness and lesion permeability is highly non-linear; a small increase in the surface layer thickness can lead to a marked decrease in permeability [32].

The purpose of this study was to look at the dependence of the dehydration dynamics of lesions due to fluorosis at 1450 and 1950 nm on the lesion depth and surface zone thickness measured with microCT.

2. MATERIALS AND METHODS

2.1 Tooth Samples and MicroCT

Sixteen posterior teeth were collected with fluorosis on the buccal and lingual surfaces. Teeth were collected from patients in the San Francisco Bay area with approval from the UCSF Committee on Human Research. The teeth were sterilized using gamma radiation and stored in 0.1% thymol solution to maintain tissue hydration and prevent bacterial growth. Samples were mounted in black orthodontic resin in order to facilitate repeatable imaging angle and orientation. The teeth were imaged using Microcomputed X-ray tomography (μCT) with a 10-μm resolution. A Scanco μCT 50 from Scanco USA (Wayne, PA) located at the UCSF Bone Imaging Core Facility was used to acquire the images. Image analysis and lesion structural measurements were carried out using Dragonfly from ORS (Montreal, Canada).

2.2 Visible/Color Images

A USB digital microscope, Model 5MP Edge AM7915MZT, AnMO Electronics Corp. (New Taipei City, Taiwan) equipped with a visible polarizer was used to acquire visible images of all samples. The digital microscope captures 5 mega-pixel (2952 × 1944) color images. Eight white LED lights contained in the camera illuminate the sample and a single polarization element is utilized to reduce glare.

2.3 SWIR Reflectance Measurements

Samples were stored in a moist environment to preserve internal hydration and the samples were immersed in a water bath before mounting and performing measurements. A computer-controlled air nozzle with a 1 mm aperture and an air pressure set to 25 psi was positioned 5 cm away at a 20° angle above the sample plane as shown in Fig. 1.

A Xenics (Leuven, Belgium) Model Xeva−2.35–320 extended range InGaAs camera sensitive from 900–2350 nm (320×240 pixel) was used to acquire the SWIR images. The camera was equipped with a Navitar f=35-mm SWIR optimized (f/1.4) lens and a 60 mm achromat lens was positioned 40 mm from the 35 mm lens. A high extinction polarizer

was used to acquire cross polarization images from 1500–2350 nm. The quantum efficiency peaks at 1500 nm near 65% and drops off rapidly to 30% after 1700 nm and drops off again to below 20% after 2000 nm. A Model SLS202 extended wavelength tungsten-halogen light source from Thorlabs (Newton, NJ) with a peak output at 1500 nm and collimating optics and a high extinction polarizer was used. A bandpass filter at 1460 nm (85) was used. A polarized, broadband amplified spontaneous emission (ASE) light source Model AP-ASE-2000 from AdValue Photonics (Tucson, AZ) with a center wavelength of 1959 nm and a bandwidth of ~100 nm (−3 dB), 230 nm (−30 dB) and an output power of 11 mW was used for the 1950 nm light source. The light sources were placed at 20° angles to the camera as shown in Fig. 1 but positioned on the same side. Images were processed and automatically analyzed using a dedicated program constructed with LabVIEW software.

3. RESULTS AND DISCUSSION

Figure 2 shows visible and SWIR reflectance images at two time points during dehydration at 1950 nm and a cross section of the microCT image showing the hypomineralization at the tooth surface. Almost all the lesions due to fluorosis show a distinct surface zone of higher mineral content near the tooth surface. The lesion shown in Fig. 2 has a uniform surface zone across the lesion. There is a lower lesion area that is deeper than the rest of the lesion. Figs. 2 B & C show the reflectance images 0 and 45 seconds after initiating dehydration. The shape of the dehydration curves appear similar to those of arrested lesions due to caries albeit with a lower overall intensity. The mean curve for intensity vs time is plotted in Fig. 3 for the sixteen areas measured. In addition the mean curves for five sound and ten active and arrested lesions due to caries from Tressel et al. [33] are plotted as well for comparison. Similar shape parameters describing the rate of intensity change during dehydration ΔI, OGR and $\%I_{fin}$ that were described by Tressel et al. [33] to fit the dehydration of caries lesions at SWIR wavelengths were used to fit the curves for the lesions due to fluorosis. Those parameters were compared to the lesion depth and the surface zone thickness measured using microCT. The mean surface zone thickness was 118 ± 30 μm and ranged from 80 – 200 μm and the lesion depth ranged from 180 to 500 μm with a mean depth of 284 ± 105 μm for the areas of fluorosis investigated. The lesion contrast after drying is plotted vs the lesion depth in Fig. 4. There was no correlation of the lesion contrast with the lesion depth or severity. In addition, the change in contrast with drying (ΔI) is plotted in Fig. 4 against the surface zone thickness measured with microCT. There was no correlation of ΔI with the surface zone thickness. In addition, there was no correlation of the other parameters, the overall growth rate (OGR) and fraction of the intensity change that takes place in the tail of the curve ($\%I_{fin}$) with the lesion depth or surface zone thickness for either 1450 or 1950 nm.

In a previous study comparing the rate of intensity change during dehydration for simulated caries lesions with thickness of the surface zone we found that a thin surface zone of only 10–20 μm caused large changes and all the surface zones measured in this study were greater than 80 μm in thickness [32]. Therefore, these results are not surprising. Lee et al. [20] attempted to use SWIR imaging from 1300–1700 nm to discriminate between lesions due to caries and lesions due to hypomineralization and found that the lesions due to fluorosis behaved similarly to arrested lesions due to caries. Multiple attempts have been

made utilizing SWIR reflectance measurements during dehydration and optical coherence tomography to develop methods for differentiating caries lesions from developmental defects. It appears that arrested lesions due to caries and lesions due to fluorosis have very similar dehydration dynamics that preludes differentiating them using SWIR reflectance imaging. SWIR imaging methods and optical coherence tomography appear to have great potential for assessing their severity [7, 18, 19]

ACKNOWLEDGEMENTS

The authors would like to acknowledge Jacob Simon and Cynthia Darling and support from NIDCR/NIH grant R01-DE0228295.

REFERENCES

[1]. Fejerskov O, Nyvad B, and Kidd E, Dental Caries: The Disease and its Clinical Management Wiley Blackwell, (2015).

[2]. Beltran-Aguilar ED, Barker LK, Canto MT, Dye BA, Gooch BF, Griffin SO, Hyman J, Jaramillo F, Kingman A, Nowjack-Raymer R, Selwitz RH, and Wu T, “Surveillance for dental caries, dental sealants, tooth retention, edentulism, and enamel fluorosis--United States, 1988–1994 and 1999–200,” MMWR Surveill Summ, 54(3), 1–43 (2005).

[3]. Angmar-Mansson B, de Josselin de Jong E, Sundstrom F, and ten Bosch JJ, “Strategies for improving the assessment of dental fluorosis: focus on optical techniques,” Adv Dent Res, 8(1), 75–9 (1994). [PubMed: 7993563]

[4]. Li SM, Zou J, Wang Z, Wright JT, and Zhang Y, “Quantitative assessment of enamel hypomineralization by KaVo DIAGNOdent at different sites on first permanent molars of children in China,” Pediatr Dent, 25(5), 485–90 (2003). [PubMed: 14649613]

[5]. McGrady MG, Ellwood RP, Taylor A, Maguire A, Goodwin M, Boothman N, and Pretty IA, “Evaluating the use of fluorescent imaging for the quantification of dental fluorosis,” BMC Oral Health, 12, 47 (2012). [PubMed: 23116324]

[6]. Pretty IA, McGrady M, Zakian C, Ellwood RP, Taylor A, Sharif MO, Iafolla T, Martinez-Mier EA, Srisilapanan P, Korwanich N, Goodwin M, and Dye BA, “Quantitative light fluorescence (QLF) and polarized white light (PWL) assessments of dental fluorosis in an epidemiological setting,” BMC Public Health, 12, 366 (2012). [PubMed: 22607363]

[7]. Hirasuna K, Fried D, and Darling CL, “Near-IR imaging of developmental defects in dental enamel.,” J Biomed Opt, 13(4), 044011:1–7 (2008). [PubMed: 19021339]

[8]. Darling CL, Huynh GD, and Fried D, “Light scattering properties of natural and artificially demineralized dental enamel at 1310-nm,” J Biomed Opt, 11(3), 034023 (2006).

[9]. Chan KH, and Fried D, “Multispectral cross-polarization reflectance measurements suggest high contrast of demineralization on tooth surfaces at wavelengths beyond 1300-nm due to reduced light scattering in sound enamel ” J Biomed Opt, 23(6), 060501 (2018).

[10]. Chung S, Fried D, Staninec M, and Darling CL, “Multispectral near-IR reflectance and transillumination imaging of teeth ” Biomed Opt Express, 2(10), 2804–2814 (2011). [PubMed: 22025986]

[11]. Ng C, Almaz EC, Simon JC, Fried D, and Darling CL, “Near-infrared imaging of demineralization on the occlusal surfaces of teeth without the interference of stains,” J Biomed Opt, 24(3), 036002 (2019).

[12]. Fried WA, Chan KH, Fried D, and Darling CL, “High contrast reflectance imaging of simulated lesions on tooth occlusal surfaces at near-ir wavelengths,” Lasers Surg Med, 45(8), 533–541 (2013). [PubMed: 23857066]

[13]. Simon JC, Chan KH, Darling CL, and Fried D, “Multispectral near-IR reflectance imaging of simulated early occlusal lesions: variation of lesion contrast with lesion depth and severity,” Lasers Surg Med, 46(3), 203–15 (2014). [PubMed: 24375543]

[14]. Simon JC, Lucas SA, Lee RC, Staninec M, Tom H, Chan KH, Darling CL, and Fried D, "Near-IR transillumination and reflectance imaging at 1300-nm and 1500-1700-nm for in vivo caries detection," Lasers Surg Med, 48(6), 828–836 (2016). [PubMed: 27389018]

[15]. Wu J, and Fried D, "High contrast near-infrared polarized reflectance images of demineralization on tooth buccal and occlusal surfaces at 1310-nm," Lasers Surg Med, 41(3), 208–13 (2009). [PubMed: 19291753]

[16]. Zakian C, Pretty I, and Ellwood R, "Near-infrared hyperspectral imaging of teeth for dental caries detection," J Biomed Opt, 14(6), 064047–7 (2009). [PubMed: 20059285]

[17]. Fried WA, Abdellaziz M, Darling CL, and Fried D, "High Contrast Reflectance Imaging of Enamel Demineralization and Remineralization at 1950-nm for the Assessment of Lesion Activity," Lasers Surg Med, 53(7) 968–977 (2021). [PubMed: 33442896]

[18]. Kashirtsev F, Simon JC, and Fried D, "Imaging dental fluorosis at SWIR wavelengths from 1300 to 2000-nm," Photonic Therapeutics and Diagnostics in Dentistry, Head and Neck Surgery, and Otolaryngology. Proc. SPIE, Vol. 11627 0Q:1–6 (2021).

[19]. Kashirtsev F, Tressel J, Simon JC, and Fried D, "High contrast imaging of dental fluorosis in the short wavelength infrared (SWIR) " J Biophotonics, in press, (2021).

[20]. Lee RC, Jang AT, and Fried D, "Near-infrared imaging of enamel hypomineralization due to developmental defects," Lasers in Dentistry XXIII. Proc. SPIE, Vol. 10044 08:1–4 (2017).

[21]. Kaneko K, Matsuyama K, and Nakashima S, "Quantification of Early Carious Enamel Lesions by using an Infrared Camera," Early detection of Dental caries II. Indiana University press, 483–99 (1999).

[22]. Zakian CM, Taylor AM, Ellwood RP, and Pretty IA, "Occlusal caries detection by using thermal imaging," J Dent, 38(10), 788–795 (2010). [PubMed: 20599464]

[23]. Usenik P, Burmen M, Fidler A, Pernus F, and Likar B, "Near-infrared hyperspectral imaging of water evaporation dynamics for early detection of incipient caries," J Dent, 42(10), 1242–7 (2014). [PubMed: 25150104]

[24]. Ando M, Stookey GK, and Zero DT, "Ability of quantitative light-induced fluorescence (QLF) to assess the activity of white spot lesions during dehydration," Am J Dent, 19(1), 15–8 (2006). [PubMed: 16555651]

[25]. Ando M, Ferreira-Zandona AG, Eckert GJ, Zero DT, and Stookey GK, "Pilot clinical study to assess caries lesion activity using quantitative light-induced fluorescence during dehydration," J Biomed Opt, 22(3), 35005 (2017). [PubMed: 28280839]

[26]. Lee RC, Darling CL, and Fried D, "Assessment of remineralization via measurement of dehydration rates with thermal and near-IR reflectance imaging," J Dent, 43, 1032–1042 (2015). [PubMed: 25862275]

[27]. Lee RC, Staninec M, Le O, and Fried D, "Infrared methods for assessment of the activity of natural enamel caries lesions," IEEE J Sel Top Quant Elect, 22(3), 6803609 (2014).

[28]. Lee RC, Darling CL, and Fried D, "Activity assessment of root caries lesions with thermal and near-infrared imaging methods," J Biophotonics, 10(3), 433–445 (2016). [PubMed: 27060450]

[29]. Stookey GK, "Quantitative light fluorescence: A technology for early monitoring of the caries process," Dent Clin North Am, 49(4), 753–70(2005). [PubMed: 16150315]

[30]. Lee C, Lee D, Darling CL, and Fried D, "Nondestructive assessment of the severity of occlusal caries lesions with near-infrared imaging at 1310 nm," J Biomed Opt, 15(4), 047011 (2010). [PubMed: 20799842]

[31]. Lee RC, Darling CL, and Fried D, "Assessment of remineralized dentin lesions with thermal and near-infrared reflectance imaging," Laser in Dentistry XXII. Proc. SPIE, Vol. 9692 0B1–5 (2016).

[32]. Chang NN, Jew JM, and Fried D, "Lesion dehydration rate changes with the surface layer thickness during enamel remineralization," Lasers in Dentistry XXIV. Proc. SPIE, Vol. 10473 0D:1–7 (2018).

[33]. Tressel J, Abdelaziz M, and Fries D, "Dynamic SWIR Imaging near the 1950 nm water absorption band for caries lesion diagnosis," J Biomed Opt 26(5), 056006 (2021).

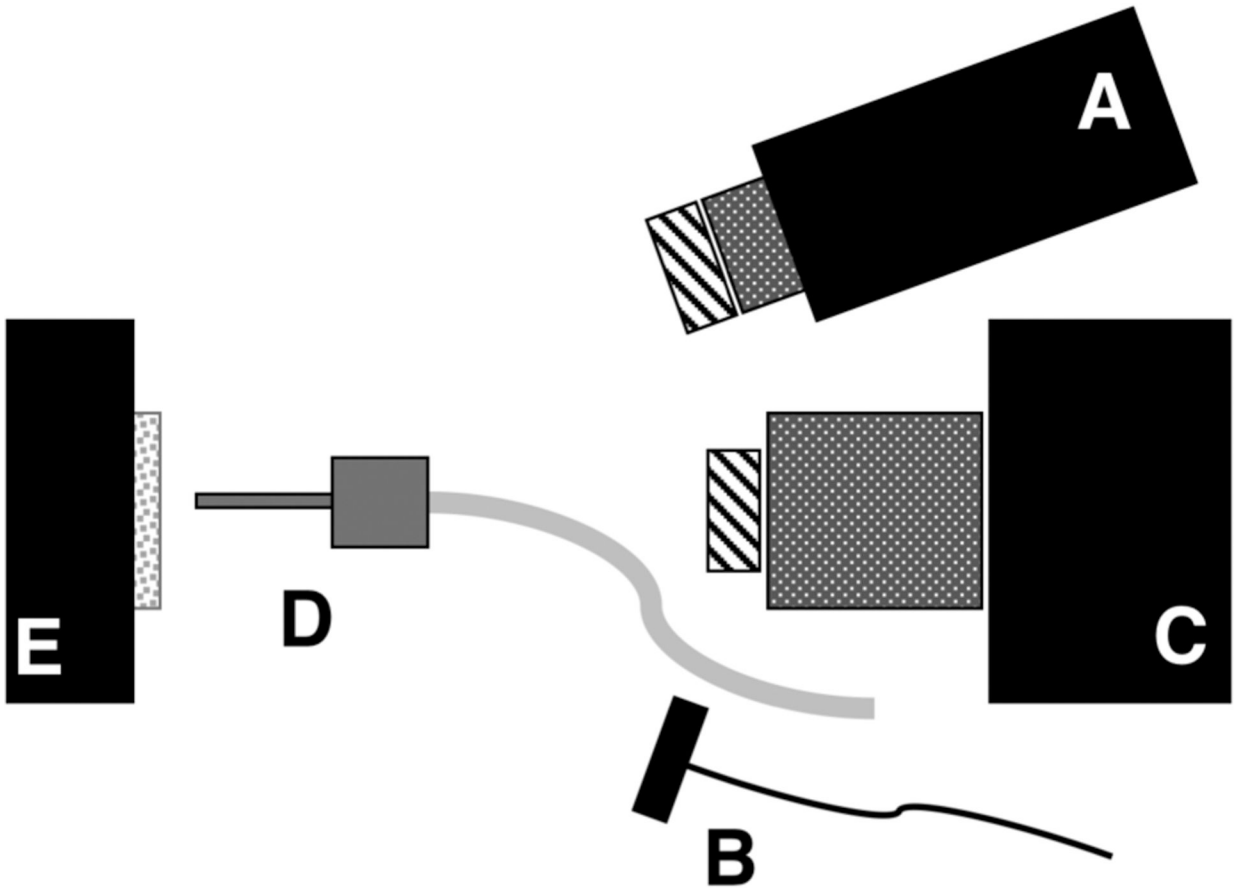

Fig. 1.

Schematic of the experimental setup showing (A) tungsten-halogen light source with bandpass filters, collimating lens and polarizer, (B) polarized 1950 nm fiber optic light source, (C) Xenics extended range InGaAs camera with lens and polarizer, (D) air nozzle and (E) tooth samples mounted on XYZ stage. Light sources A & B were positioned on the same side for these measurements.

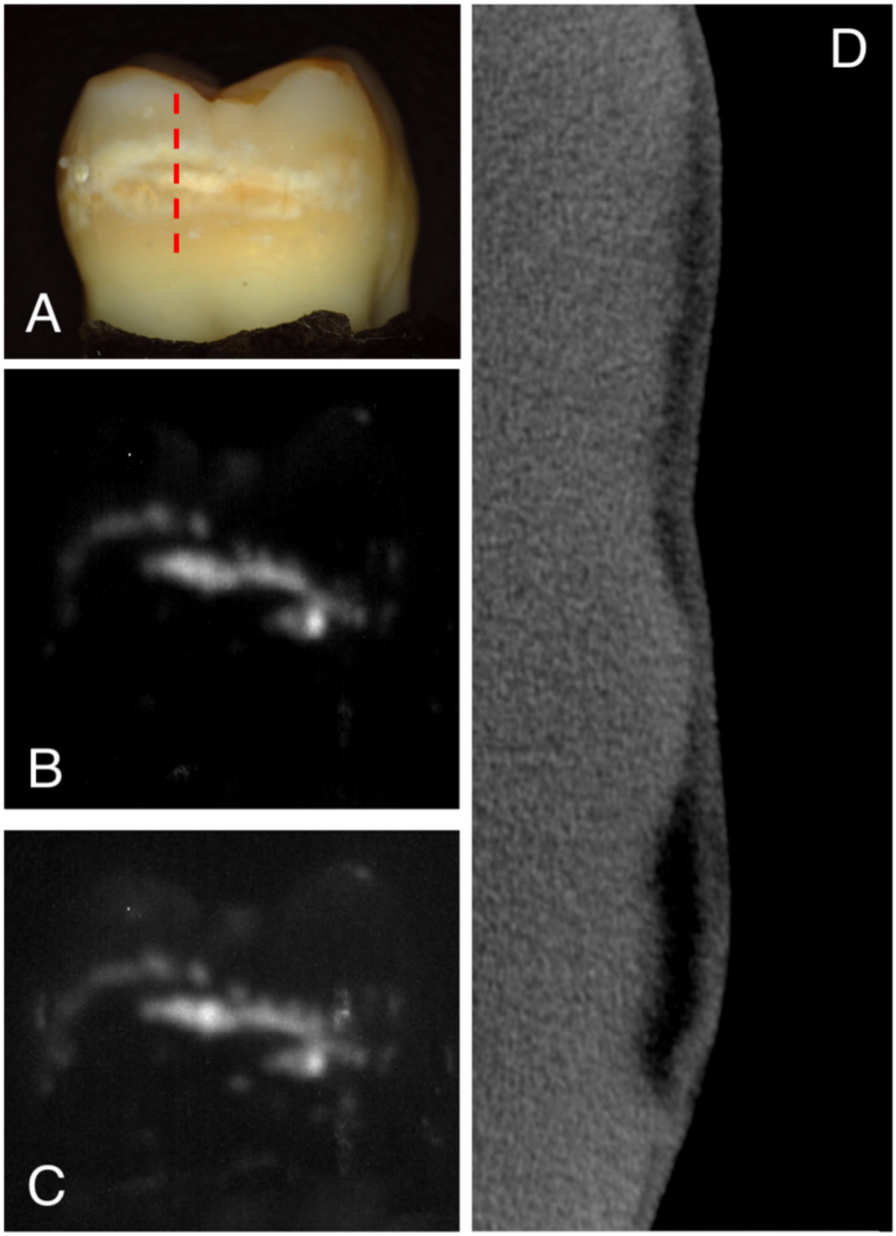

Fig. 2.

(A) Color image of a sample tooth with fluorosis on the crown. (B & C) SWIR reflectance images at 1950 nm at 0 and 45 seconds of dehydration. (D) MicroCT image extracted at the position of the red dotted line in (A) showing the mineral density profile from the tooth surface.

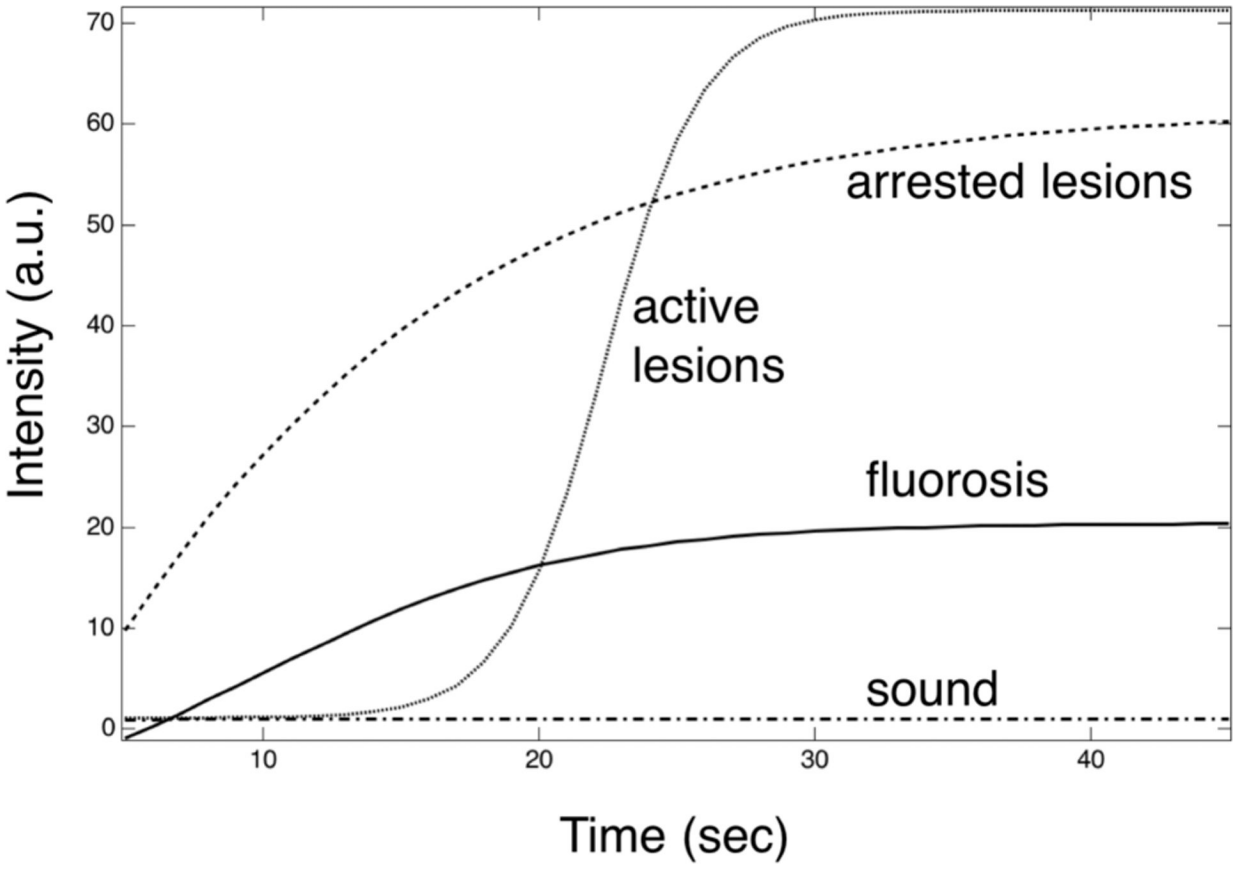

Fig. 3.

Mean intensity vs time curves plotted for sound, active and arrested lesions (Ref 33) and the areas of fluorosis during dehydration at 1950 nm for the 16 samples from this study.

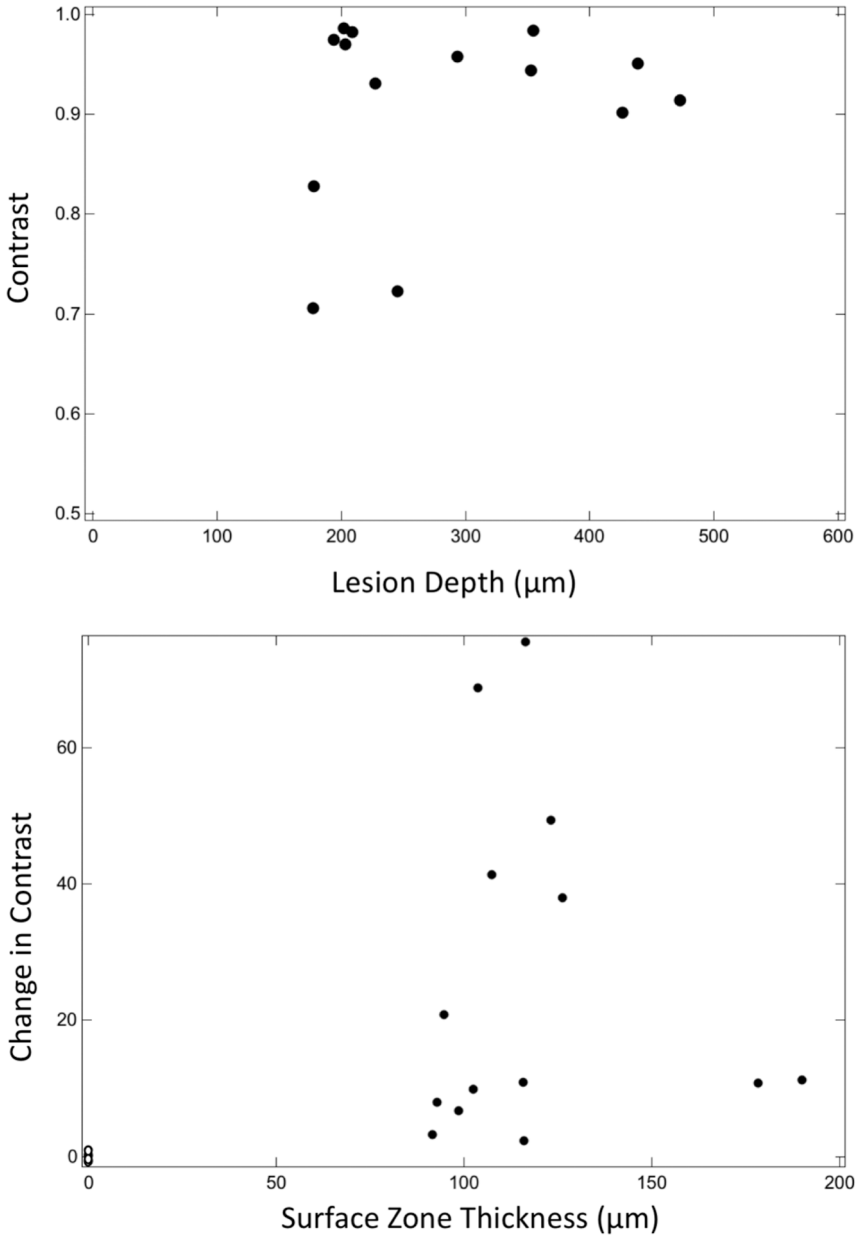

Fig. 4.

Plots of the (Top) contrast of hypomineralization at 1950 nm vs the depth of hypomineralization and (bottom) change in the contrast of hypomineralization at 1950 nm vs the surface zone thickness for selected locations on the 16 samples.